Supporting Information

Doping Gd_{16} Nanoclusters for Expanded Optical Properties and Thermometry Application

Tingting Li,[a] Jinyu Liu,[a] Feng Jiang,[b] Shengrong He,[b] Jinzhe Liu,[a] Weinan Dong,[b] Ying Zhang,*[c,d] Yanan Li*[c,d] and Zhennan Wu*[b]

[a] School of Materials Science and Engineering, Jilin Jianzhu University, Changchun 130018, China.

[b] State Key Laboratory of Integrated Optoelectronics and College of Electronic Science and Engineering, Jilin University, Changchun 130012, China.

[c] Department of Pediatrics, Children's Medical Center, The First Hospital of Jilin University, Changchun 130021, China.

[d] Clinical Research Center for Child Health, the First Hospital of Jilin University, Changchun 130021, China.

Correspondence: *yingzhang@jlu.edu.cn*; *ynli@jlu.edu.cn*; *wuzn@jlu.edu.cn*

Experimental and theoretical intensity parameters.

The theoretical background of 4f-4f intensity theory is well established and widely used in the lanthanides, especially in trivalent europium and terbium compounds.[1-4]The intensities of 4f-4f transitions in Eu^{3+} and Tb^{3+} complexes are usually expressed in terms of the areas under the curves in their emission spectra. From these spectra, the experimental intensity parameters Ω_2, Ω_4, and Ω_6 may be estimated using the following equation:[5, 6]

$$\frac{A_{ed}}{A_{md}} = \frac{\int I_J(v)dv}{\int I_{md}(v)dv} = \frac{e^2}{S_{md}} \frac{v_J^3}{9n^2} (n^2+2)^2 \sum_{\lambda} \Omega_\lambda \langle {}^7F_J \| U^\lambda \| {}^5D_{(0,4)} \rangle^2 (\lambda = 2,4) \quad \text{S1}$$

where A_{ed} and A_{md} on the left of the equation are the electric dipole transition and magnetic dipole transition rate, respectively, and their ratio can be acquired by calculating the corresponding emission spectra integrated area ratio. On the right of the equation, magnetic line strength S_{md} (Eu^{3+}) = 7.83×10^{-42} cm^{-1}, e = 1.6×10^{-19} C, n is the refractive index of the medium (n ≈ 1.5 for most Eu^{3+} samples). $\langle {}^7F_J \| U^\lambda \| {}^5D_0 \rangle^2$ are equal to 0.0032, 0.0023 and 0.00023 for λ = 2，4 and 6，respectively.

Intramolecular Energy Transfer Rates Calculation. The intramolecular energy transfer (IET) rates from the ligands to Ln^{3+} ion was calculated by taking into account the dipole-dipole ($W_{d\text{-}d}$), dipole–multipole ($W_{d\text{-}m}$), and exchange (W_{ex}) mechanisms on JOYSpectra web platform.[7-11]

$$W_{d-d} = \frac{S_L (1-\sigma_1)^2 4\pi e^2}{(2J+1) G \hbar R_L^6} \sum_{\lambda} \Omega_\lambda^{FED} \langle \Psi' J' \| U^{(\lambda)} \| \Psi J \rangle^2 F \quad \text{S2}$$

$$W_{d-m} = \frac{S_L}{(2J+1)G} \frac{2\pi e^2}{\hbar} \sum_{\lambda} (\lambda+1) \frac{\langle r^\lambda \rangle^2}{\left(R_L^{\lambda+2}\right)^2} \langle f \| C^{(\lambda)} \| f \rangle^2 (1-\sigma_\lambda)^2 \times \langle \Psi' J' \| U^{(\lambda)} \| \Psi J \rangle^2 F$$

S3

$$W_{ex} = \frac{(1-\sigma_0)^2 8\pi e^2}{(2J+1) G \hbar R_L^4} \langle \Psi' J' \| U^{(\lambda)} \| \Psi J \rangle^2 \sum_{m} \left\| \left\langle \Phi \left| \sum_j \mu_z(j) S_m(j) \right| \Phi^* \right\rangle \right\|^2 F \quad \text{S4}$$

where RL is the donor-acceptor states distance, Ω_λ^{FED} are the intensity parameters assigned exclusively with the forced electric dipole mechanism (Table S14, S15). The values of the squared reduced matrix elements $\langle \Psi' J' \| U^{(\lambda)} \| \Psi J \rangle^2$, which depend only on the Ln^{3+} ion, were taken from Carnall et al. SL is the dipole strength of the ligand transition involved in IET (~10^{-36} and ~10^{-40} $(esu)^2 \cdot cm^2$ for S1 and T1, respectively), the $\langle r^\lambda \rangle$ are the 4f radial integrals, G is the ligand state degeneracy (G = 1 or 3 for S1 or T1, respectively), $\langle f \| C^{(\lambda)} \| f \rangle$ (f = 3) is the reduced matrix element of Racah's tensor

operators, and $(1 - \sigma_\lambda)$ is the shielding factors that have a relation with the overlap integrals between valence orbitals of the pair Ln–X (X is the ligating atom in the first coordination sphere).[12]

In Eq. S4, S_m is the spin operator in the ligand and μz is the dipole operator (its z-component), the value of the element matrix of these coupled operators is ~10^{-36} $(esu)^2 \cdot cm^2$.[13] The $\langle \Psi' J' \| U^{(\lambda)} \| \Psi J \rangle$ is the reduced matrix elements of the lanthanide spin operator, which were calculated by using free-ion wavefunctions in the intermediate coupling scheme.[14]

The F term in the above equations is the spectral overlap factor that considers the energy mismatch condition between donor and acceptor states. For the case of ligand-to-Ln^{3+} energy transfer, F can be estimated by Eq. S5:

$$F = \frac{1}{\hbar\gamma_L}\sqrt{\frac{\ln(2)}{\pi}}e^{-\left(\frac{\Delta}{\hbar\gamma_L}\right)^2 ln(2)} \quad \text{S5}$$

where Δ is the energy difference between the donor state and the lanthanide ion acceptor state, $\Delta = E_{lig} - E_{Ln}$. The γL is the bandwidth at half-height of the donor states (S1 and T1), which is assumed here to have a typical value of γL = 3000 cm^{-1} for both S1 and T1 states.[15]

The forward energy transfer rates (W) involving the Ln^{3+} ions as acceptors are calculated by the sum over Eq. S2, S3, and S4 in the same pathway:

$$W = W_{d-d} + W_{d-m} + W_{ex} \quad \text{S6}$$

W must be multiplied by the barrier factor exp $(-|\Delta|/k_B T)$ only if Δ is negative, where k_B is the Boltzmann constant and T is the temperature. The same expressions and considerations are used to calculate the backward IET rates W_b (the energy transfer rates from the Ln^{3+} ion to the ligand states). The calculated values of forward and backward IET rates are given in Table S3-S10.

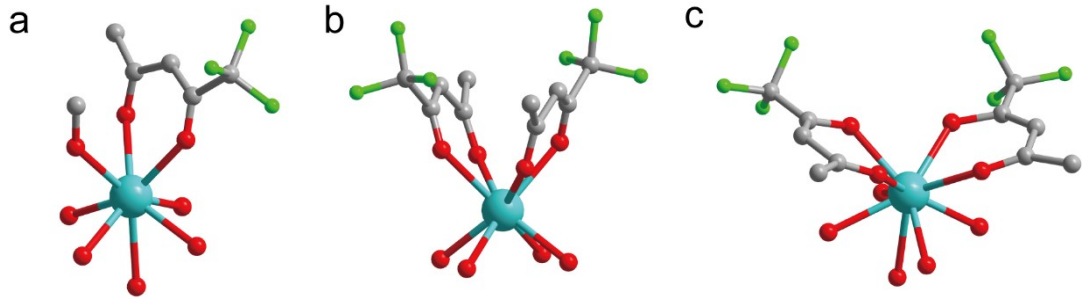

Figure S1. The ligands and methanol molecules exhibit three different coordination environments.

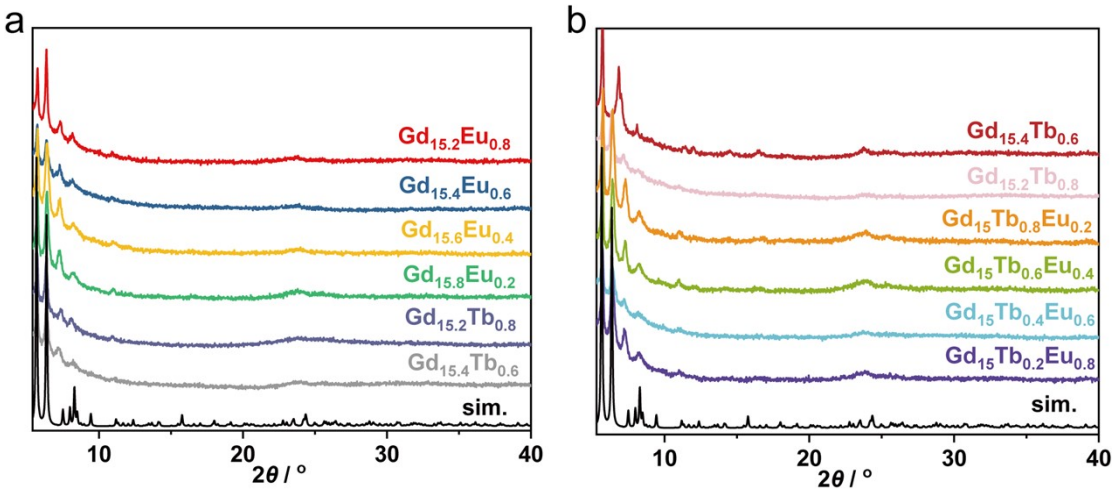

Figure S2. PXRD of compound $Gd_{16-x}Eu_x$, $Gd_{16-x}Tb_x$ and $Gd_{15}Tb_{1-x}Eu_x$(x=0.2, 0.4, 0.6, 0.8).

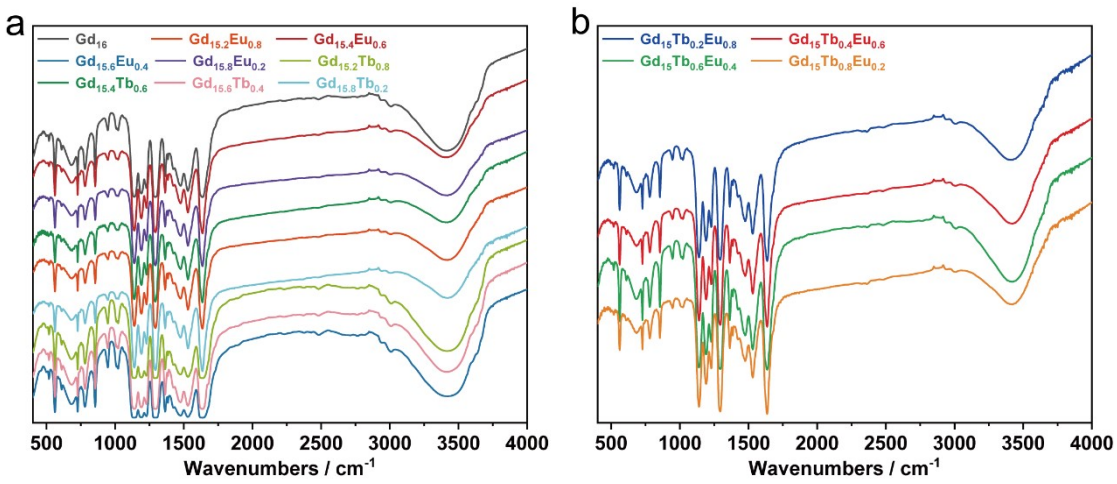

Figure S3. Infrared spectrum of PXRD of compound $Gd_{16-x}Eu_x$, $Gd_{16-x}Tb_x$ and $Gd_{15}Tb_{1-x}Eu_x$(x=0.2, 0.4, 0.6, 0.8).

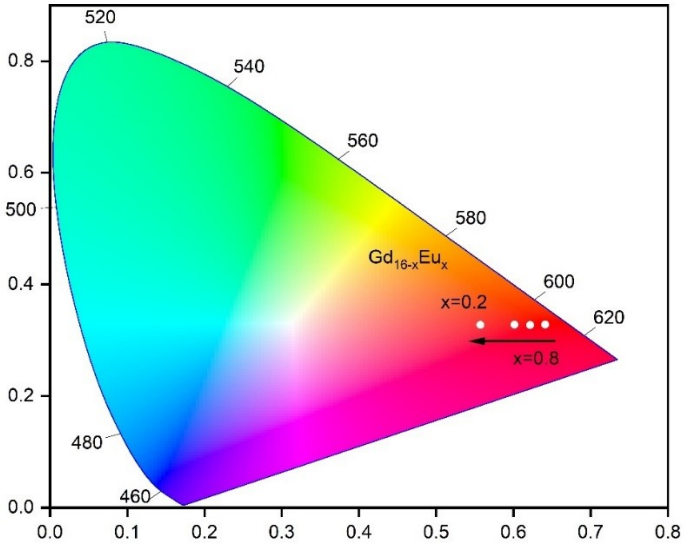

Figure S4. CIE chromaticity diagrams of $Gd_{16-x}Eu_x$ (x = 0.2, 0.4, 0.6, 0.8).

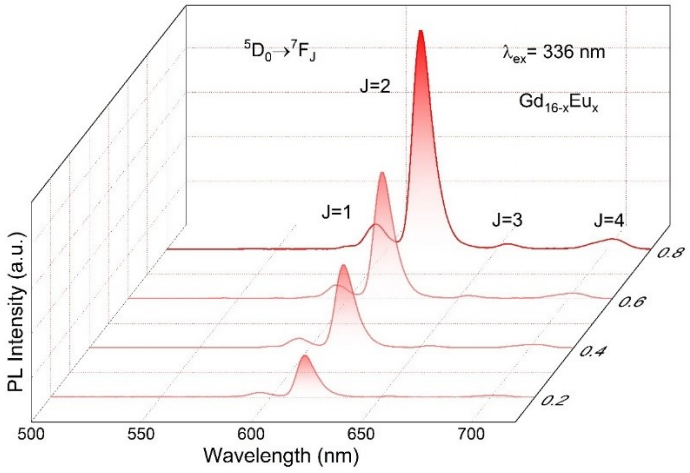

Figure S5. Emission spectra of Gd_{16} doped with europium at different concentrations

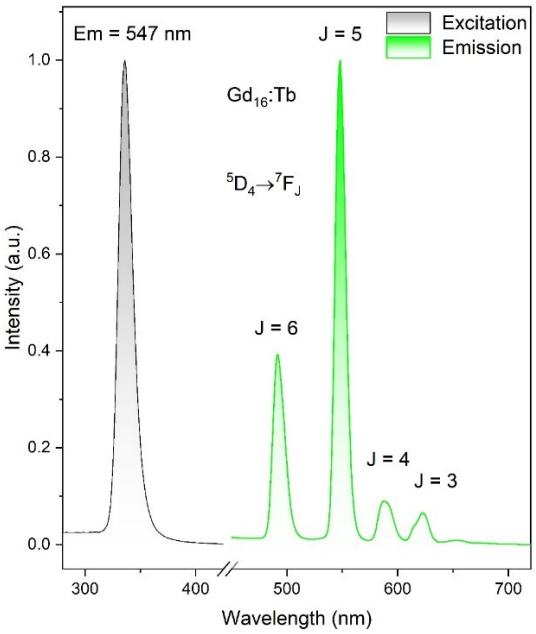

Figure S6. Excitation and emission spectra of Tb^{3+} ion doped Gd_{16}.

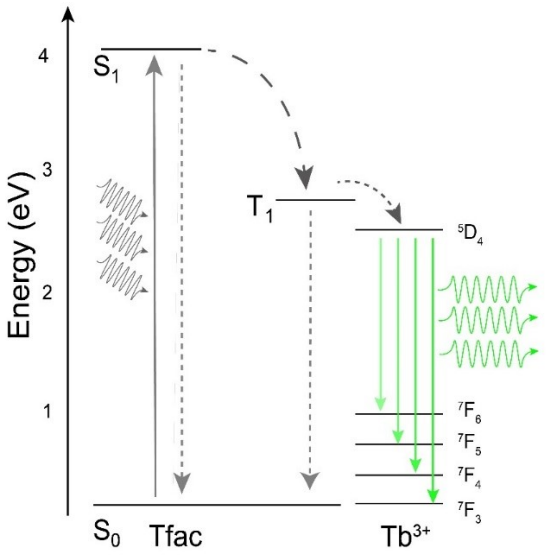

Figure S7. Mechanism diagram of luminescence of Tb^{3+} ions sensitized by ligands.

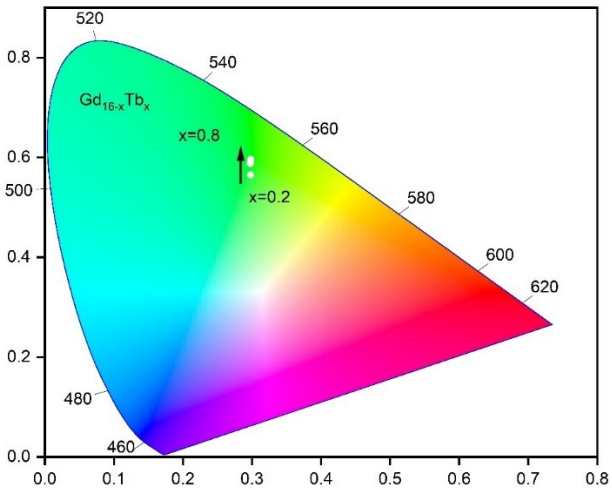

Figure S8. CIE chromaticity diagram of $Gd_{16-x}Tb_x$ (x = 0.2, 0.4, 0.6, 0.8) clusters.

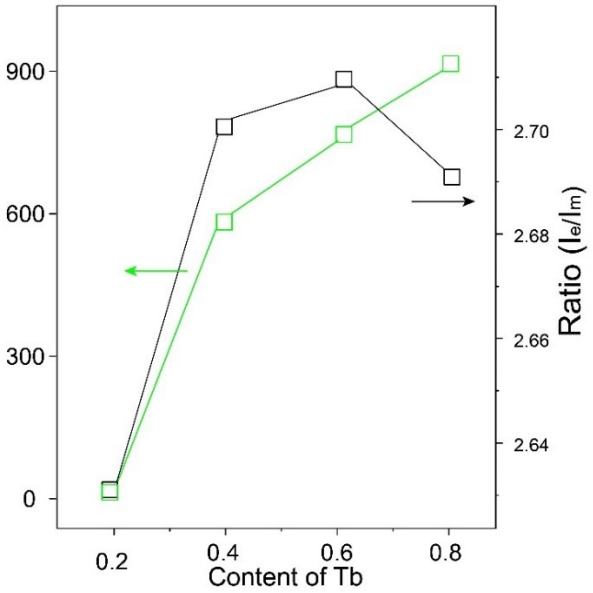

Figure S9. Photoluminescence of Tb^{3+} ion depends on concentration and coordination environment.

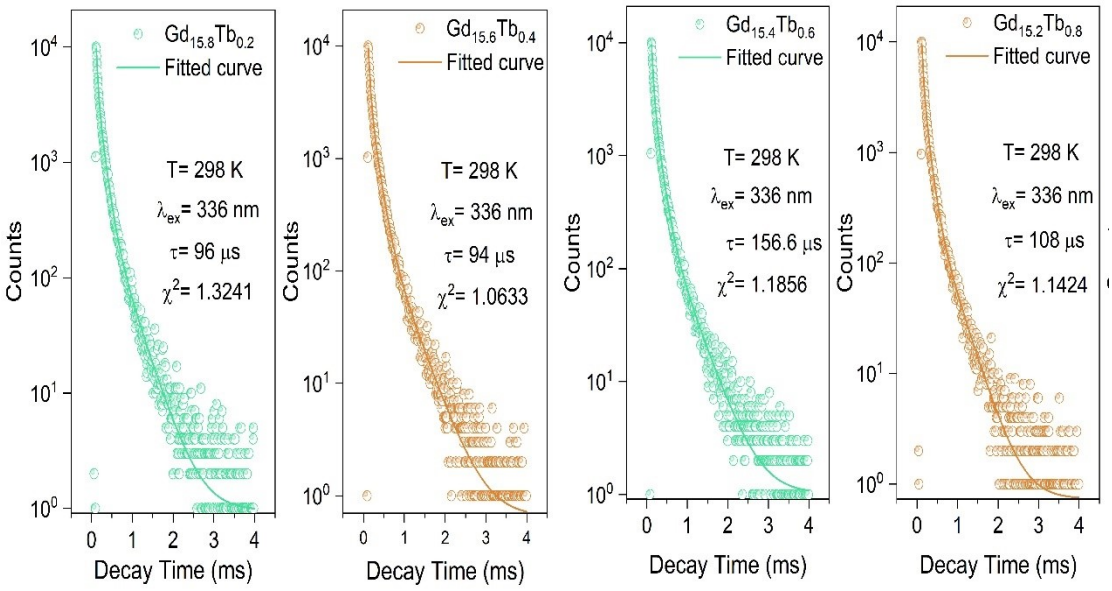

Figure S10. Emission decay of Tb^{3+} ion at 547 nm in $Gd_{16-x}Tb_x$ (x = 0.2, 0.4, 0.6, 0.8) cluster.

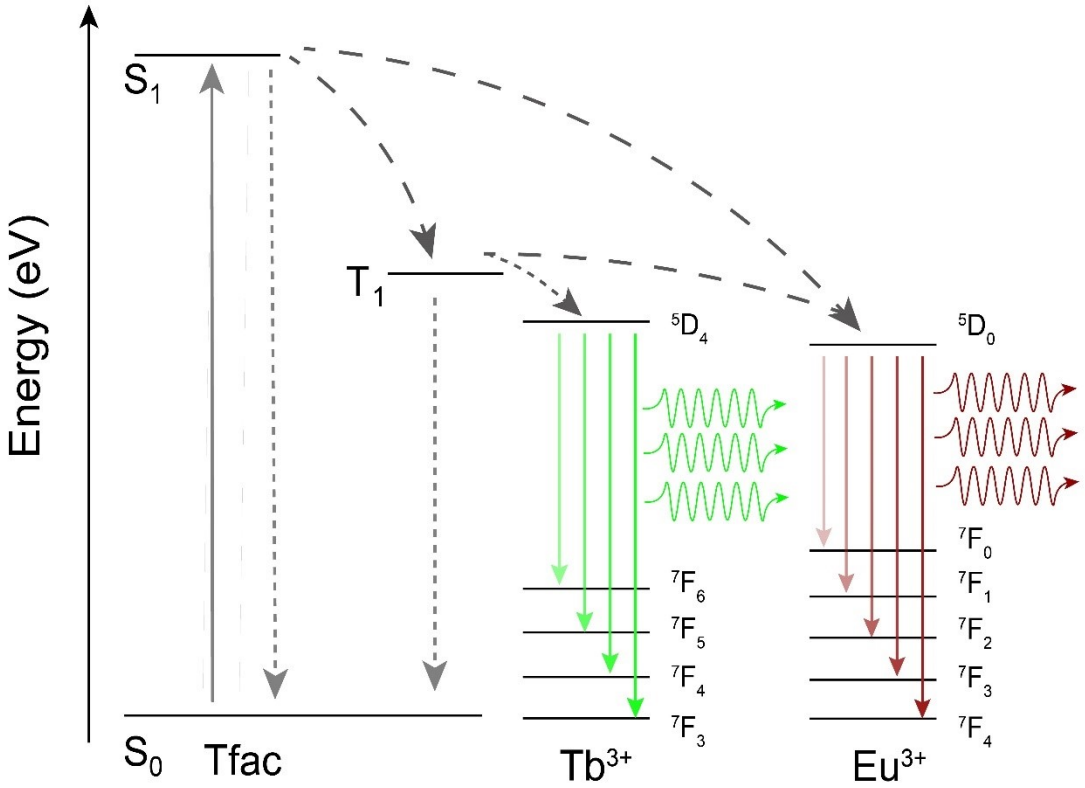

Figure S11. Tb^{3+} ion to Eu^{3+} ion energy transfer excitation diagram.

Table S1. ICP data for all samples (What is given in the table is the atomic content ratio in the sample).

Sample	Theoretical	Experimental
$Gd_{15.8}Eu_{0.2}$	79.0:1	79.0:1
$Gd_{15.6}Eu_{0.4}$	39.0:1	39.0:1
$Gd_{15.4}Eu_{0.6}$	26.0:1	26.6:1
$Gd_{15.2}Eu_{0.8}$	19.0:1	20.1:1
$Gd_{15.8}Tb_{0.2}$	79.0:1	79.0:1
$Gd_{15.6}Tb_{0.4}$	39.0:1	39.0:1
$Gd_{15.4}Tb_{0.6}$	26.0:1	26.9:1
$Gd_{15.2}Tb_{0.8}$	19.0:1	19.4:1
$Gd_{15}Tb_{0.2}Eu_{0.8}$	100:1:5	100:1:5
$Gd_{15}Tb_{0.4}Eu_{0.6}$	100:3:4	100:3:3
$Gd_{15}Tb_{0.6}Eu_{0.4}$	100:4:3	100:3:3
$Gd_{15}Tb_{0.8}Eu_{0.2}$	100:5:1	100:5:1

Table S2. Forward (W^T) and backward (WT B) IET rates (in s^{-1}) for $Gd_{15.2}Eu_{0.8}$ and $Gd_{15.4}Eu_{0.6}$.

Clusters	W^T	WT B
$Gd_{15.2}Eu_{0.8}$	$3.3233\times10^7\ s^{-1}$	$3.23\times10^6\ s^{-1}$
$Gd_{15.4}Eu_{0.6}$	$3.0114\times10^7\ s^{-1}$	$3.53\times10^6\ s^{-1}$

Table S3. $Gd_{15.4}Eu_{0.6}$: S_1 to Eu^{3+} IET rates (in s^{-1}). The Δ is the energy difference (in cm^{-1}) between the donor and the acceptor state, W (%) is the percentual contribution of the pathway, W is the sum of the dipole-dipole (W_{d-d}), the dipole-multipole (W_{d-m}), and the exchange (W_{ex}) mechanisms.

Pathway	Transition	Δ(cm^{-1})	W (%)	W	W_{d-d}	W_{d-m}	W_{ex}
32	$^7F_1\rightarrow{}^5G_2$	2480.0	47.93	3.52E+06	0.00E+00	0.00E+00	3.52E+06
7	$^7F_0\rightarrow{}^5D_1$	9473.0	41.19	3.02E+06	0.00E+00	0.00E+00	3.02E+06
18	$^7F_0\rightarrow{}^5D_4$	914.0	5.59	4.10E+05	3.32E-05	4.10E+05	0.00E+00
28	$^7F_1\rightarrow{}^5D_2$	7389.0	2.1	1.54E+05	0.00E+00	0.00E+00	1.54E+05
26	$^7F_1\rightarrow{}^5D_0$	11579.0	1.72	1.26E+05	0.00E+00	0.00E+00	1.26E+05

Table S4. $Gd_{15.4}Eu_{0.6}$: Eu^{3+} to S_1 IET rates (in s^{-1}). The Δ is the energy difference (in cm^{-1}) between the donor and the acceptor state, W (%) is the percentual contribution of the pathway, W is the sum of the dipole-dipole (W_{d-d}), the dipole-multipole (W_{d-m}), and the exchange (W_{ex}) mechanisms.

Pathway	Transition	Δ(cm^{-1})	W (%)	W	W_{d-d}	W_{d-m}	W_{ex}
18	$^7F_0\rightarrow{}^5D_4$	-914.0	88.9	6.64E+02	5.37E-08	6.64E+02	0.00E+00
32	$^7F_1\rightarrow{}^5G_2$	-2480.0	10.8	8.06E+01	0.00E+00	0.00E+00	8.06E+01

Table S5. $Gd_{15.4}Eu_{0.6}$: T_1 to Eu^{3+} IET rates (in s^{-1}). The Δ is the energy difference (in cm^{-1}) between the donor and the acceptor state, W (%) is the percentual contribution of

the pathway, W is the sum of the dipole-dipole (W_{d-d}), the dipole-multipole (W_{d-m}), and the exchange (W_{ex}) mechanisms.

Pathway	Transition	Δ(cm^{-1})	W (%)	W	W_{d-d}	W_{d-m}	W_{ex}
7	$^7F_0 \rightarrow {}^5D_1$	3773.0	88.01	2.65E+07	0.00E+00	0.00E+00	2.65E+07
26	$^7F_1 \rightarrow {}^5D_0$	5879.0	10.38	3.13E+06	0.00E+00	0.00E+00	3.13E+06
28	$^7F_1 \rightarrow {}^5D_2$	1689.0	1.61	4.84E+05	0.00E+00	0.00E+00	4.84E+05

Table S6. $Gd_{15.4}Eu_{0.6}$: Eu^{3+} to T_1 IET rates (in s^{-1}). The Δ is the energy difference (in cm^{-1}) between the donor and the acceptor state, W (%) is the percentual contribution of the pathway, W is the sum of the dipole-dipole (W_{d-d}), the dipole-multipole (W_{d-m}), and the exchange (W_{ex}) mechanisms.

Pathway	Transition	Δ(cm^{-1})	W (%)	W	W_{d-d}	W_{d-m}	W_{ex}
32	$^7F_1 \rightarrow {}^5G_2$	3220.0	99.99	3.53E+06	0.00E+00	0.00E+00	3.53E+06

Table S7. $Gd_{15.2}Eu_{0.8}$: S_1 to Eu^{3+} IET rates (in s^{-1}). The Δ is the energy difference (in cm^{-1}) between the donor and the acceptor state, W (%) is the percentual contribution of the pathway, W is the sum of the dipole-dipole (W_{d-d}), the dipole-multipole (W_{d-m}), and the exchange (W_{ex}) mechanisms.

Pathway	Transition	Δ(cm^{-1})	W (%)	W	W_{d-d}	W_{d-m}	W_{ex}
32	$^7F_1 \rightarrow {}^5G_2$	2680.0	50.45	3.36E+06	0.00E+00	0.00E+00	3.36E+06
7	$^7F_0 \rightarrow {}^5D_1$	9673.0	38.4	2.56E+06	0.00E+00	0.00E+00	2056E+06
18	$^7F_0 \rightarrow {}^5D_4$	1114.0	6.05	4.03E+05	1.88E-05	4.03E+05	0.00E+00
28	$^7F_1 \rightarrow {}^5D_2$	7589.0	2.03	1.36E+05	0.00E+00	0.00E+00	1.36E+05
26	$^7F_1 \rightarrow {}^5D_0$	11779.0	1.54	1.03E+05	0.00E+00	0.00E+00	1.03E+05

Table S8. $Gd_{15.2}Eu_{0.8}$: Eu^{3+} to S_1 IET rates (in s^{-1}). The Δ is the energy difference (in cm^{-1}) between the donor and the acceptor state, W (%) is the percentual contribution

of the pathway, W is the sum of the dipole-dipole (W_{d-d}), the dipole-multipole (W_{d-m}), and the exchange (W_{ex}) mechanisms.

Pathway	Transition	$\Delta(cm^{-1})$	W (%)	W	W_{d-d}	W_{d-m}	W_{ex}
18	$^7F_0 \rightarrow {}^5D_4$	-1114.0	89.16	2.48E+02	1.16E-08	2.48E+02	0.00E+00
32	$^7F_1 \rightarrow {}^5G_2$	-2680.0	10.54	2.94E+01	0.00E+00	0.00E+00	2.94E+01

Table S9. $Gd_{15.2}Eu_{0.8}$: T_1 to Eu^{3+} IET rates (in s^{-1}). The Δ is the energy difference (in cm^{-1}) between the donor and the acceptor state, W (%) is the percentual contribution of the pathway, W is the sum of the dipole-dipole (W_{d-d}), the dipole-multipole (W_{d-m}), and the exchange (W_{ex}) mechanisms.

Pathway	Transition	$\Delta(cm^{-1})$	W (%)	W	W_{d-d}	W_{d-m}	W_{ex}
7	$^7F_0 \rightarrow {}^5D_1$	3473.0	87.57	2.91E+07	0.00E+00	0.00E+00	2.91E+07
26	$^7F_1 \rightarrow {}^5D_0$	5579.0	10.91	3.63E+06	0.00E+00	0.00E+00	3.63E+06
28	$^7F_1 \rightarrow {}^5D_2$	1389.0	1.51	5.03E+05	0.00E+00	0.00E+00	5.03E+05

Table S10. $Gd_{15.2}Eu_{0.8}$: Eu^{3+} to T_1 IET rates (in s^{-1}). The Δ is the energy difference (in cm^{-1}) between the donor and the acceptor state, W (%) is the percentual contribution of the pathway, W is the sum of the dipole-dipole (W_{d-d}), the dipole-multipole (W_{d-m}), and the exchange (W_{ex}) mechanisms.

Pathway	Transition	$\Delta(cm^{-1})$	W (%)	W	W_{d-d}	W_{d-m}	W_{ex}
32	$^7F_1 \rightarrow {}^5G_2$	3520.0	99.93	3.23E+06	0.00E+00	0.00E+00	3.23E+06

Table S11. Experimental and theoretical 4f–4f intensity parameters Ω_λ (10^{-20} cm^2) ($\lambda = 2,4$) for $Gd_{15.2}Eu_{0.8}$ and $Gd_{15.4}Eu_{0.6}$. The FED contributions (to be used in the calculations of the energy transfer rates for the dipole-dipole mechanism) are in parentheses.

Sample	Experimental		Theoretical	
	Ω_2	Ω_4	$\Omega_2^{theo}(\Omega_2^{FED})$	$\Omega_4^{theo}(\Omega_4^{FED})$
$Gd_{15.2}Eu_{0.8}$	0.98900	1.31900	0.989012	0.000896

$Gd_{15.4}Eu_{0.6}$	1.58300	2.23200	1.583001	0.001294

Table S12. Doubly reduced matrix elements used in the calculations of the dipole strengths for absorption and emission of $Gd_{16-x}Eu_x$ (x = 0.6, 0.8).

Transition	Element	Value	Transition	Element	Value
$^5D_2 \leftarrow {}^7F_0$	$\langle \psi \Vert U^2 \Vert \psi' \rangle$	0.0008	$^5D_0 \rightarrow {}^7F_2$	$\langle \psi \Vert U^2 \Vert \psi' \rangle$	0.0032
$^5L_6 \leftarrow {}^7F_1$	$\langle \psi \Vert U^6 \Vert \psi' \rangle$	0.0090	$^5D_0 \rightarrow {}^7F_4$	$\langle \psi \Vert U^4 \Vert \psi' \rangle$	0.0023
$^5L_6 \leftarrow {}^7F_0$	$\langle \psi \Vert U^6 \Vert \psi' \rangle$	0.0155	$^5D_0 \rightarrow {}^7F_6$	$\langle \psi \Vert U^6 \Vert \psi' \rangle$	0.0002
$^5D_4 \leftarrow {}^7F_0$	$\langle \psi \Vert U^4 \Vert \psi' \rangle$	0.0011			

Table S13. Fluorescence lifetime and transfer efficiency of $Gd_{16-x}Tb_x$ and $Gd_{15}Tb_{1-x}Eu_x$ (x = 0.2, 0.4, 0.6, 0.8).

Cluster	Lifetime(μs)	Cluster	Lifetime(μs)	Efficiency
$Gd_{15.8}Tb_{0.2}$	96	$Gd_{15}Tb_{0.2}Eu_{0.8}$	85	11.5%
$Gd_{15.6}Tb_{0.4}$	94	$Gd_{15}Tb_{0.4}Eu_{0.6}$	84	10.7%
$Gd_{15.4}Tb_{0.6}$	156.6	$Gd_{15}Tb_{0.6}Eu_{0.4}$	146.4	7%
$Gd_{15.2}Tb_{0.8}$	108	$Gd_{15}Tb_{0.8}Eu_{0.2}$	103	5%

Table S14. Best-fitting parameters for the thermometric parameter (Δ).

	$Gd_{15}Tb_{0.2}Eu_{0.8}$	$Gd_{15}Tb_{0.8}Eu_{0.2}$
A_1	0.354	7.121
A_2	-0.003	0.182
x_0	232.540	233.220
R^2	0.993	0.997

Table S15 Single Crystal Structure date of Gd_{16}.

Compound	Gd_{16}
CCDC number	2100059
Formula	$Gd_{16}C_{108}O_{74}F_{60}H_{136}$
*M*r	6274.1
Crystal system	monoclinic
Space group	C_2/m
a /Å	21.8785(7)
b / Å	23.5682(5)
c / Å	20.7294(6)
α / °	90
β / °	107.857(3)
γ / °	90
V/Å^3	10173.9(5)
Z	2
*D*c/g cm^{-3}	2.048
μ/mm^{-1}	34.248
Data/params	9619/711
*2*θ range/°	7.502-143.324
Obs reflns	28707
GOOFs	1.109
$R_1[I>2\sigma(I)]^a$	0.1060
wR_2(All data)^b	0.2838

References

1. Y. Zhang, X. Wang, K. Xu, F. Zhai, J, Shu, Y. Tao, J. Wang, L. Jiang, L. Yang, Y. Wang, W. Liu, J. Su, Z. Chai and S. Wang, *J. Am. Chem. Soc.* 2023, **145**, 24, 13161-13168.
2. B. G. Wybourne, *J. Opt. Soc. Am.*, 1965, **55**, 928-935.
3. C. Görller-Walrand and K. Binnemans, *Handb. Phys. Chem. Rare Earths*, 1998, **25**, 101-264.
4. G. F. de Sá, O. L. Malta, C. de Mello Donegá, A. M. Simas, R. L. Longo, P. A. Santa-Cruz and E. F da Silva Jr, *Coord. Chem. Rev*, 2000, **196**, 165-195.
5. X. Li, X. Shen, M. Lu, J. Wu, Y. Zhong, Z. Wu, W. W. Yu, Y. Gao, J. Hu and J. Zhu, *Angew. Chem*, 2023, **135**, e202217832.
6. A. N. C. Neto, E. E. S. Teotonio, G. F. de Sá, H. F. Brito, J. Legendziewicz, L. D. Carlos, M. C. F. C. Felinto, P. Gawryszewska, R. T. Moura Jr and R. L. Longo, W. M. Faustino, O. L. Malta, *Handb. Phys. Chem. Rare Earths*, 2019, **56**, 55-162.
7. O. L. Malta, *J. Lumin*, 1997, **71**, 229-236.
8. O. L. Malta and F. R. G. e Silva, *Spectrochim. Acta, Part A*, 1998, **54**, 1593-1599.
9. R. Longo, F. R. G. e Silva and O. L. Malta, *Chem. Phys. Lett*, 2000, **328**, 67-74.
10. O. L. Malta, *J. Non-Cryst. Solids*, 2008, **354**, 4770-4776.
11. A. N. C. Neto and R. T. Moura Jr, *Chem. Phys. Lett*, 2020, **757**, 137884.
12. F. R. G. e Silva and O. L. Malta, *J. Alloys Compd*, 1997, **250**, 427-430.
13. G. S. Ofelt, *J. Chem. Phys*, 1963, **38**, 2171-2180.
14. E. Kasprzycka, A. N. C. Neto, V. A. Trush, L. Jerzykiewicz, V. M. Amirkhanov, O. L. Malta, J. Legendziewicz and P. Gawryszewska, *J. Rare Earths*, 2020, **38**, 552-563.
15. E. E. S. Teotonio, H. F. Brito, G. F. de Sá, M. C. F. C. Felinto, R. H. A. Santos, R. M. Fuquen, I. F. Costa, A. R. Kennedy, D. Gilmore and W. M. Faustino, *Polyhedron*, 2012, **38**, 58-67.